



Published in final edited form as:

Cancer Cell. 2012 November 13; 22(5): 656–667. doi:10.1016/j.ccr.2012.08.027.

Crosstalk between ROR1 and the pre-B-Cell Receptor Promotes Survival of t(1;19) Acute Lymphoblastic Leukemia

Vincent T. Bicocca^{1,2}, Bill H. Chang^{2,3}, Behzad Kharabi Masouleh⁴, Markus Muschen^{4,5}, Marc M. Loriaux^{2,6}, Brian J. Druker^{1,2,7}, and Jeffrey W. Tyner^{2,8,*}

¹Division of Hematology and Medical Oncology, Oregon Health & Science University, Portland, Oregon 97239, USA

²Knight Cancer Institute, Portland, Oregon 97239, USA

³Division of Pediatric Hematology and Oncology, Department of Pediatrics, Oregon Health & Science University, Portland, OR 97239, USA

⁴Childrens Hospital Los Angeles and Leukemia and Lymphoma Program, Norris Comprehensive Cancer Center, University of Southern California, Los Angeles, CA 90027, USA

⁵Department of Laboratory Medicine, University of California San Francisco, San Francisco, California 94143, USA

⁶Department of Pathology, Oregon Health & Science University, Portland, Oregon 97239, USA

⁷Howard Hughes Medical Institute, Portland, OR 97239, USA

⁸Department of Cell & Developmental Biology, Oregon Health & Science University, Portland, OR 97239, USA

SUMMARY

We report that t(1;19)-ALL cells universally exhibit expression of and dependence on the cell surface receptor, ROR1. We further identify t(1;19)-ALL cell sensitivity to the kinase inhibitor dasatinib due to its inhibition of the pre-B-cell receptor (pre-BCR) signaling complex. These phenotypes are a consequence of developmental arrest at an intermediate/late stage of B-lineage maturation. Additionally, inhibition of pre-BCR signaling induces further ROR1 upregulation, and we identify distinct ROR1 and pre-BCR downstream signaling pathways that are modulated in a counter-balancing manner—both leading to AKT phosphorylation. Consistent with this, AKT phosphorylation is transiently eliminated after dasatinib treatment, but is partially restored following dasatinib potentiation of ROR1 expression. Consequently, ROR1 silencing accentuates dasatinib killing of t(1;19)-ALL cells.

INTRODUCTION

Acute lymphoblastic leukemia (ALL) is the most common form of childhood malignancy, accounting for 25% of all childhood cancers. Although great strides have been made in the

© 2012 Elsevier Inc. All rights reserved.

*Correspondence: Jeffrey W. Tyner, OHSU Knight Cancer Institute, BRB 511, Mailcode L592, 3181 SW Sam Jackson Park Road, Portland, OR 97239. Phone: (503) 346-0603; Fax: (503) 494-3688; tynerj@ohsu.edu.

Publisher's Disclaimer: This is a PDF file of an unedited manuscript that has been accepted for publication. As a service to our customers we are providing this early version of the manuscript. The manuscript will undergo copyediting, typesetting, and review of the resulting proof before it is published in its final citable form. Please note that during the production process errors may be discovered which could affect the content, and all legal disclaimers that apply to the journal pertain.

treatment of childhood leukemia, close to 20% of patients will have resistant disease eventually leading to death. To improve outcomes for these patients, it is critical to develop new therapeutic strategies that specifically target the cellular processes causing malignancy. This necessitates a comprehensive knowledge of the gene targets driving oncogenesis in each patient. From both a biological and clinical standpoint, tyrosine kinases represent an important gene family for interrogation since tyrosine kinases have been implicated in the genesis of a wide variety of malignancies, including certain subsets of ALL, and tyrosine kinase inhibitors are already in clinical use with remarkable outcomes (Krause and Van Etten, 2005). Unfortunately, most ALL patients still present without knowledge of the specific tyrosine kinases that are operationally important in disease pathogenesis. As such, we have performed functional profiling to identify tyrosine kinase targets in ALL patients.

One of the most common, recurring translocations found in ALL patients is t(1;19) (q23;p13), which is observed in approximately 5% of all pediatric ALL cases as well as 1–2% of adult ALL cases. Greater than 90% of patients with t(1;19) exhibit blasts with expression of cytoplasmic immunoglobulin heavy-chain μ (Ig μ) and an absence of CD34 on the cell surface, indicating that t(1;19) blasts are typically arrested at a later stage of B-cell differentiation (large/small pre-BII) compared with most other ALL subsets (Hunger, 1996; Williams et al., 1984). The 1;19 translocation results in the fusion transcription factor complex *E2A-PBX1* (Hunger et al., 1991; Kamps et al., 1991), which has been shown to induce myeloid, T-lymphoid, and B-lymphoid malignancies in mouse models (Bijl et al., 2005; Dederá et al., 1993; Kamps and Baltimore, 1993; Kamps et al., 1991).

RESULTS

ROR1 is a therapeutic gene target in t(1;19) ALL

To identify tyrosine kinase gene targets in ALL patients, we tested clinical specimens from pediatric ALL patients by gene-silencing with an siRNA library that collectively targets the tyrosine kinome. Cells were electroporated with pre-validated siRNAs that individually target each tyrosine kinase as well as non-specific control siRNA (Tyner et al., 2009; Tyner et al., 2008). After four days in culture, cells were subjected to an MTS assay for assessment of cell viability. Evaluation of the t(1;19)-positive sample 07-112 revealed hypersensitivity to siRNA targeting the receptor tyrosine kinase ROR1 (Figures 1 and S1A). Other ALL cases with normal karyotype (sample 08-026 is used as an example), did not exhibit sensitivity to ROR1 silencing (Figure S1B). Further evaluation by RT-PCR revealed overexpression of ROR1 in sample 07-112 at levels comparable to artificial ROR1 overexpression in Ba/F3 cells, while sample 08-026 did not exhibit detectable ROR1 expression (Figure S1C).

ROR1 expression and functional dependence is universal in t(1;19) ALL

To test whether the ectopic expression of ROR1 observed in t(1;19) patient 07-112 was uniformly detectable in all t(1;19) ALL samples, we obtained ten pediatric ALL samples (generously provided by the Children's Oncology Group ALL Biology Lab) and two cell lines that are positive for t(1;19) and compared them with five pediatric ALL samples and two cell lines that are t(1;19)-negative. We observed that all t(1;19)-positive samples exhibited ROR1 overexpression while none of the t(1;19)-negative samples or normal white blood cells displayed the same phenotype (Figures 2A and S2A). Overexpression of ROR1 protein was also observed by immunoblot and FACS analysis on t(1;19)-positive cells (Figures 2B and 2C).

To assess the extent and exclusivity of ROR1 expression in a larger cohort of patient samples, we examined microarray meta-analysis data generated from pediatric ALL patients

and normal B-cell progenitors (Trageser et al., 2009). We compared t(1;19) ALL patients with those carrying t(9;22) (*BCR-ABL*), t(12;21) (*ETV6-RUNX1*), or patients with MLL (11q23) gene rearrangements. In addition, we evaluated ROR1 levels in distinct, normal B-lineage progenitor populations (CD34⁺ Lin⁻, pro-B, pre-BI, pre-BII large, pre-BII small, and immature B cells). We observed higher levels of ROR1 expression on every t(1;19) patient compared with all patients from each of the other leukemic subsets. Similarly, t(1;19) patients showed higher levels of ROR1 expression compared with normal B-cell progenitor populations at the earliest stages of B-lineage development (CD34⁺ Lin⁻, pro-B, and pre-BI). However, when compared with normal B-lineage cells at an intermediate stage of B-cell development (large/small pre-BII and immature B), we observed high levels of ROR1, similar to those seen on t(1;19) cells (Figure 2D). These results support recent findings showing ROR1 cell surface expression on intermediate stages of normal B-cell development (Broome et al., 2011; Hudecek et al., 2010). Importantly, these and other studies did not observe ROR1 expression on normal, mature B-cells or plasma cells (Baskar et al., 2008; Fukuda et al., 2008; Hudecek et al., 2010). Hence, in non-malignant B-lineage cells, ROR1 expression appears to be absent at the earliest stages of development, becomes highly expressed at intermediate/late stages, and is then downregulated in normal, mature B-cells. Interestingly, the vast majority of blasts from t(1;19) patients are arrested at this intermediate/late stage of B-lineage development (large/small pre-BII). Hence, these data suggest that high ROR1 expression in t(1;19) may be a product of the comparatively mature differentiation state of these malignant blasts and may not be due to aberrant transcription profiles of the chimeric transcription factor E2A-PBX1. Subsequent examination of the E2A-PBX1 transcription factor in t(1;19) cell lines supports this hypothesis, since siRNA mediated knockdown of E2A-PBX1 in the t(1;19) cell line RCH-ACV showed a corresponding knockdown of the E2A-PBX1 transcriptional target WNT16B (McWhirter et al., 1999), but had no effect on expression of ROR1 (Figure S2B).

Since the two t(1;19) cell lines, RCH-ACV and Kasumi-2, recapitulated the ROR1 expression profile observed in t(1;19)-positive primary specimens, we next tested whether these cell lines were also sensitive to ROR1 silencing, as we observed with sample 07-112. We treated both cell lines as well as the control t(1;19)-negative cell line REH with siRNA specific for ROR1. Consistent with the results from sample 07-112, both RCH-ACV and Kasumi-2 cells were sensitive to ROR1 silencing (Figure 2E). Loss of ROR1 resulted in reduced cell growth and increased apoptosis (Figure S2C). In addition, treatment of RCH-ACV cells with 3 individual siRNA duplexes that target different portions of the ROR1 open reading frame as well as 3 individual siRNA duplexes that target different portions of the ROR1 3'-untranslated region (UTR) resulted in reductions of RCH-ACV cell viability that were always proportional to the respective silencing capacity of each siRNA duplex (Figure S2D and S2E). Similarly, stable overexpression of an open reading frame (ORF)-only ROR1 construct in RCH-ACV cells rescued cell viability when treated with an siRNA duplex targeting the ROR1 3'-UTR (Figure 2F), confirming the siRNA-mediated killing of t(1;19) cells is due to a ROR1-specific phenomenon. We next confirmed that this finding was reproducible in early passage t(1;19) cells propagated by xenograft into NOD/SCID mice. Xenograft cells derived from four t(1;19) patients were tested for ROR1 overexpression as well as for sensitivity to ROR1 siRNA. We found that both features were recapitulated in these early passage t(1;19) xenograft cells (Data for one representative cell line shown in Figures 2G and 2H).

ROR1 expression is regulated by pre-BCR signaling

We next wanted to investigate the functional role for ROR1 in t(1;19) ALL cells. Since upregulation of ROR1 in both malignant and normal B-cell precursors occurs at the pre-BII stage, we first examined a possible connection with other biological events known to occur

at this same stage of B-lineage maturation. One of the hallmarks of the pre-BII stage is the assembly and expression of the pre-BCR complex (Figure S3A). As such, we next examined the possibility of a functional connection between ROR1 and the pre-BCR. We tested two possibilities, 1) ROR1 directly interacts with the pre-BCR complex or 2) pre-BCR signaling may drive ROR1 expression. We began by examining ROR1 immunoprecipitates from t(1;19) ALL cells, but found no evidence for interaction of ROR1 with Ig μ or other constituents of the pre-BCR (Figure S3B). Next, we examined whether disruption of the pre-BCR would result in decreased ROR1 expression. To disrupt pre-BCR signaling we utilized siRNA against the immunoglobulin alpha and beta (Ig α and Ig β) components of the pre-BCR complex, which have previously been shown to be necessary for pre-BCR activity (Papavasiliou et al., 1995; Teh and Neuberger, 1997). As expected, knockdown of Ig α or Ig β resulted in significantly impaired t(1;19) ALL cell viability, which was amplified with simultaneous silencing of both proteins (Figure 3A). We then analyzed ROR1 expression following inhibition of the pre-BCR by knockdown of Ig α/β . Paradoxically, knockdown of Ig α and Ig β did not inhibit ROR1 expression, and instead resulted in significant ROR1 upregulation (Figure 3B).

The unexpected upregulation of ROR1 after pre-BCR silencing suggested a functional connection between ROR1 and the pre-BCR, with ROR1 upregulation after pre-BCR inhibition potentially representing an intrinsic response mechanism to perturbation of the pre-BCR pathway. We next examined a pharmacological approach to inhibition of pre-BCR signaling, employing the inhibitor dasatinib, which has been previously described to block mature-BCR signaling (McCaig et al., 2011). Similar to siRNA mediated disruption of the pre-BCR, inhibition of pre-BCR signaling with dasatinib resulted in impaired viability and increased apoptosis of the pre-BCR-positive t(1;19) ALL cell lines RCH-ACV and Kasumi-2, while the pre-BCR-negative t(12;21) ALL cell line REH was insensitive (Figure 3C and 3D). As with knockdown of Ig α/β , dasatinib mediated pre-BCR inhibition resulted in further upregulation of ROR1 mRNA and protein (Figure 3E and 3F; Figure S3C). To confirm that ROR1 upregulation is not a general response to all apoptotic stimuli in t(1;19) cells, we treated RCH-ACV cells with doxorubicin, which induces apoptosis through the p53 pathway and is a therapeutic agent used in the setting of ALL. We observed robust induction of apoptosis in response to doxorubicin (Figure S3D), however, ROR1 was not upregulated and, in fact, exhibited reduced expression (Figure S3E). This stands in marked contrast to the robust upregulation of ROR1 observed after inhibition of the pre-BCR with dasatinib or silencing of the pre-BCR with siRNA directed against Ig α/β (Figure 3B and 3F; Figure S3C and S3E).

Dasatinib inhibited pre-BCR signaling disrupts AKT in t(1;19) ALL

The observation that dasatinib recapitulated the phenotype of pre-BCR silencing (reduction of t(1;19) ALL cell viability and ROR1 upregulation) suggested dasatinib could be a useful tool to study functional interactions between ROR1 and the pre-BCR. First, however, we wanted to validate that dasatinib was operating via inhibition of pre-BCR signaling and also identify the specific kinase targets of dasatinib in this setting. As previously described, the pre-BCR is noted for regulation of both pro-proliferation and pro-differentiation signaling required for normal B-cell differentiation and a variety of kinases play a prominent role in this signaling complex (Figure 4A). We began by examining putative dasatinib targets that are known to participate in this pre-BCR signaling complex. BTK and SRC-family kinases are established targets of dasatinib (Hantschel et al., 2007; Karaman et al., 2008) and critical components of the pre-BCR and mature BCR signaling complexes (Hsueh and Scheuermann, 2000). Indeed, phosphorylation of BTK and the SRC-family kinase, LYN, were inhibited after dasatinib exposure. The additional loss of phosphorylation of pre-BCR complex components, SYK, Ig α , and AKT (which are not direct targets of dasatinib),

indicated complete disruption of the pre-BCR signaling complex by dasatinib (Figure 4B). In addition, direct inhibition of AKT with an allosteric inhibitor of AKT (MERCK AKT1/2; published as drug #17 in Table 2 of (Bilodeau et al., 2008)) resulted in ROR1 upregulation, as was also observed with dasatinib and pre-BCR silencing (Figure 4C). These results suggested that t(1;19) ALL dasatinib sensitivity occurs due to inhibition of pre-BCR-initiated BTK and/or SRC kinases that subsequently activate AKT. However, dasatinib has the capacity to inhibit many other kinases so we wanted to further validate this hypothesis. Accordingly, we treated t(1;19) ALL cells with the SRC kinase inhibitor ponatinib (which lacks activity against BTK (O'Hare et al., 2009)) and observed a phenotype identical to dasatinib—selective sensitivity of t(1;19) ALL cells and potent reduction of AKT phosphorylation (Figure 4D and 4G). In contrast, a third kinase inhibitor, imatinib, exhibited no effect on t(1;19) ALL cells (Figure 4E). Examination of these three drugs to understand target genes inhibited by both dasatinib and ponatinib but not by imatinib revealed the only candidate gene targets to explain the dasatinib/ponatinib phenotype are SRC kinases, EPH receptor kinases, and CSK (Figure 4F). Treatment of these cells with a CSK inhibitor (BMS-599626) or a BTK inhibitor (PCI-32765) did not recapitulate the dasatinib/ponatinib phenotype, indicating that dasatinib/ponatinib sensitivity is due to SRC kinases or EPH receptor kinases (Figure 4G). Examination of EPH receptor expression revealed that EPHA3 is upregulated in t(1;19) ALL cells (Figure S4A). However, silencing of EPHA3 did not yield any discernible effect on t(1;19) ALL cell viability. No other EPH receptors exhibited aberrant expression in the t(1;19) setting, indicating that EPH receptors are likely not underlying this dasatinib/ponatinib cell viability response and suggesting SRC-family kinases as the operationally important target underlying t(1;19) ALL dasatinib sensitivity (Figure S4B).

Finally, we closely examined downstream pre-BCR signaling in the context dasatinib exposure. The pre-BCR is known to stimulate a pro-differentiation pathway (BTK/BLNK/PLC γ 2) as well as a pro-survival/proliferation, anti-differentiation pathway (PI3K/AKT) (Hashimoto et al., 1999; Herzog et al., 2009). We observed no effects on phosphorylation of BLNK/PLC γ 2 after dasatinib treatment (Figure S4C), which is consistent with our conclusion that BTK is dispensable for dasatinib-mediated t(1;19) ALL cell killing. In contrast, analysis of downstream AKT substrates revealed activation (reduced phosphorylation) of FOXO-family transcription factors, upregulation of RAG1 protein, loss of expression of the pro-survival gene BCL6, and activation (reduced phosphorylation) of pro-apoptotic BAD—all of which lead to arrested proliferation and apoptosis (Figure 3D; Figure S4D–F) (Brunet et al., 1999; Datta et al., 1997; Hideshima et al., 2010).

ROR1 drives signaling pathways that are compensatory with pre-BCR signaling

The increase of ROR1 expression after inhibition of the pre-BCR signaling complex led us to hypothesize the existence of counter-balancing pools of signaling proteins that function downstream of ROR1 or the pre-BCR in a compensatory manner to influence cell growth and viability. To evaluate this possibility, we needed to first determine the mechanism by which ROR1 influences downstream signaling pathways. We first examined the potential tyrosine kinase function of ROR1. However, we found no evidence of endogenous ROR1 tyrosine phosphorylation (Figure S6A). Likewise, *in vitro* kinase activity assays revealed no significant ROR1 kinase activity, a finding consistent with a recent study showing absence of intrinsic ROR1 kinase activity (Gentile et al., 2011). Hence, to identify alternative modalities for activation of signaling cascades by ROR1, we performed a mass spectrometry based proteomic screen of proteins associating with endogenous ROR1 in t(1;19) ALL. Using three t(1;19) ALL cell lines (Kasumi-2, 697, and RCH-ACV) we prepared ROR1 or isotype control immunoprecipitates. We analyzed these samples with mass-spectrometry to identify proteins that specifically and consistently co-immunoprecipitated with ROR1 and

not with isotype control. This approach successfully identified four candidate ROR1 interacting proteins (Table 1; Figure S5). Two of these proteins (TBC1D1 and TBC1D4) have been reported to function as RAB GTPase activating proteins (Park et al., 2011; Sano et al., 2003), suggesting regulation of small GTPase signaling as a possible avenue for ROR1 signaling.

Though this work presented a potential mechanism by which ROR1 can activate downstream signaling pathways, the specific signaling pathways regulated by ROR1 as well as the manner by which these pathways interact with the pre-BCR signaling complex remained unclear. To address these questions, we examined protein phosphorylation patterns after treatment of cells with ROR1 siRNA or with dasatinib. We observed three categories of phosphorylation changes following these treatments: 1) phosphorylation decreased by dasatinib but increased or no change by ROR1 siRNA, 2) phosphorylation increased by dasatinib but decreased or no change by ROR1 siRNA, or 3) phosphorylation reduced by both dasatinib and ROR1 siRNA (Figure 5A). Notably, the MAP kinase family members, MEK and ERK, which are regulated downstream of small GTPases such as RAS (Mendoza et al., 2011), RAB (Bhuin and Roy, 2010), and RAC (Wang et al., 2010), exhibited reduced phosphorylation following ROR1 silencing and increased phosphorylation following dasatinib treatment. In addition, phosphorylation of AKT at serine 473 was among the phosphorylation events that were reduced by both dasatinib and ROR1 siRNA. Independent immunoblotting successfully validated reduction in phosphorylation of MEK, ERK, and AKT following ROR1 silencing (Figure 5B). Since AKT was regulated by both dasatinib and ROR1, this represented a potential signaling node for functional interaction between ROR1 and the pre-BCR. Consistent with this model, phosphorylation of AKT at serine 473 is almost completely abrogated after short time points with dasatinib treatment (1 and 4 hours); however, phosphorylation is partially restored at 24 hours once ROR1 expression has been further induced (Figure 5C). In addition, ROR1 exhibited the capacity to regulate the MEK/ERK cascade, so we hypothesized that cross-talk between AKT and MEK/ERK enables ROR1 to regulate AKT and thereby cooperate with the pre-BCR signaling complex. To test this, we simultaneously treated cells with dasatinib and a MEK inhibitor, PD98059. This combination treatment resulted in sustained reduction of AKT phosphorylation, suggesting the 24-hour partial AKT recovery may, indeed, be mediated by cross-talk between MEK/ERK and AKT (Figure 5C). Finally, since STAT3 was recently described as a regulator of ROR1 expression in CLL (Li et al., 2010) and we observed increases in STAT3 phosphorylation after dasatinib exposure in t(1;19) ALL cells (Figure 5A; Figure S6A), we co-treated RCH-ACV cells with dasatinib and the STAT3 inhibitor S31-201, and we observed prevention of ROR1 upregulation in response to this drug combination (Figure S6B).

Based on the observed upregulation of ROR1 in response to pre-BCR inhibition by dasatinib and the compensatory signaling pathway driven by ROR1, we hypothesized that ROR1 may partially rescue cell survival after inhibition of the pre-BCR. If this were the case, then targeting of ROR1 in the context of dasatinib exposure would potentiate dasatinib killing of t(1;19) cells. To test this hypothesis, we treated t(1;19) ALL cell lines with non-specific-, ROR1-, or Ig α -targeting siRNA and subsequently exposed these cells to graded concentrations of dasatinib. As predicted, cells subjected to ROR1 silencing were more sensitive to dasatinib compared with cells treated with non-specific siRNA, suggesting that ROR1 can function as a rescue pathway for cell survival in the context of pre-BCR inhibition (Figure 5D). Importantly, knockdown of Ig α did not increase the level of killing when combined with dasatinib, indicating that the ROR1/dasatinib phenotype cannot be achieved by non-specific combination of any two cellular insults.

Clinical significance of dasatinib sensitivity in B-cell malignancies

To determine the clinical significance of dasatinib sensitivity in t(1;19) ALL we asked whether primary cells taken directly from ALL patients were similarly sensitive to dasatinib exposure. We tested leukemia cells from ten ALL patients of varying disease subsets over graded concentrations of dasatinib. Two of these ten patient samples were obtained from t(1;19)-positive patients and both samples tested were highly sensitive to dasatinib, with IC₅₀ values of approximately 2 and 12 nM, while the eight other ALL samples did not achieve IC₅₀ values even at the highest tested concentration (1000 nM) (Figure 6A). Importantly, examination of ROR1 levels in these two t(1;19) patients confirmed ROR1 overexpression, similar to levels observed on all other t(1;19) samples previously tested (Figure 6B).

We next utilized a xenograft model of t(1;19) ALL to examine dasatinib sensitivity in vivo. The early passage t(1;19) ALL xenograft line ICN12 showed dasatinib sensitivity in vitro at concentrations similar to those observed in patient-derived cell lines and primary samples (Figure 6C). These ICN12, t(1;19)-ALL cells were then injected into NOD/SCID mice. Following engraftment, mice were treated with a dose-escalating regimen of dasatinib or vehicle control, starting with dosages already described for Ph+ ALL (Boulos et al., 2011) and monitored for 60 days. Mice receiving dasatinib exhibited significantly prolonged survival compared with vehicle-treated control mice (Figure 6D).

Finally, since t(1;19) ALL does not represent the only B-lineage malignancy arrested at an intermediate/late stage of B-cell development, we analyzed ROR1 status and dasatinib sensitivity in additional primary cells from B-cell malignancies arrested at both the intermediate and mature stages of B-cell development. Specifically, we examined primary samples from patients diagnosed with pre-BCR-positive t(17;19) ALL (as indicated by CD34-negativity and Ig μ expression, Figures S6A and B), as well as a mature BCR-positive Burkitt's sample. Both showed high ROR1 expression levels, similar to those observed in t(1;19) ALL samples (Figure 6E). As expected, these samples were also sensitive to dasatinib treatment, with IC₅₀s comparable to t(1;19) ALL (Figure 6F). These results support the idea that ROR1 expression and dasatinib sensitivity are conserved characteristics of B-cell malignancies exhibiting both pre-BCR and mature BCR expression.

DISCUSSION

In agreement with other recent work (Broome et al., 2011; Hudecek et al., 2010), we show that ROR1 upregulation in t(1;19) ALL is a product of B-lineage development arrest at the pre-BII stage of B-cell development and not a result of aberrant regulation by the E2A-PBX1 transcription factor generated by the 1;19 translocation. Our studies also show ROR1 is upregulated in t(17;19) ALL and Burkitt's leukemia/lymphoma, suggesting ROR1 may be expressed in most B-cell malignancies arrested at an intermediate or mature stage of development. This hypothesis is supported by findings showing ROR1 expression in cell lines and primary samples derived from patients with Mantle cell lymphoma (MCL) and chronic lymphocytic leukemia (CLL) (Baskar et al., 2008; Fukuda et al., 2008; Hudecek et al., 2010). Importantly, the expression of ROR1 on cells from the mature B-lineage malignancies, CLL, MCL and Burkitt's, demonstrates a deviation from the normal distribution of ROR1-expression observed in B-cell development. While ROR1-expression is observed only in the intermediate stage of normal B-cell development, it is observed in both intermediate and mature B-cell malignancies. This important distinction suggests that retention or reactivation of ROR1-expression plays a role in maintenance of cell viability of these mature, malignant B-cell clones.

We also show that the cytoplasmic pre-BCR, present in pre-BII progenitor equivalent t(1;19) ALL, is actively stimulating the PI3K/AKT pathway, and this pathway is inhibited following pre-BCR inhibition with dasatinib. Interestingly, we find that the PI3K/AKT component of the pre-BCR pathway can also be stimulated by ROR1, and inhibition of pre-BCR signaling results in rapid upregulation of ROR1 and subsequent reactivation of AKT via ROR1/MEK/ERK signaling. Indeed, cooperation between AKT and MEK/ERK has been demonstrated during B-lineage development; likewise, cross-talk between these signaling pathways is well documented in a variety of settings (Mendoza et al., 2011). This observation raises interesting questions about a potential cooperative role for ROR1 and MEK/ERK signaling in regulating B-cell development with the pre-BCR. Supporting this idea is work that shows MEK/ERK signaling in pre-B cells can both cooperate with AKT signaling to coordinate RAG gene expression and drive pro-survival signaling (Novak et al., 2010; Taguchi et al., 2003). A pro-survival function for ROR1/MEK/ERK signaling supports our observation of impaired cell viability following ROR1 silencing in t(1;19) ALL cells, and is consistent with the idea that ROR1 is being upregulated following pre-BCR/AKT inhibition in an attempt to rescue cell viability. The potentiated effect on cell viability we observe with simultaneous ROR1 silencing and pre-BCR inhibition supports this model.

Taken together, our findings support a model in which normal B-cell progenitors upregulate ROR1 expression in coordination with assembly and signaling from the pre-BCR complex at the pre-BII large stage of development. Here, the pre-BCR drives AKT activation, which inhibits differentiation, drives proliferation and promotes survival. ROR1 activated MEK/ERK signaling cooperates with AKT to support convergent pro-survival pathways (Figure 7A) (Novak et al., 2010). As normal pre-B cells transition to immature B cells, the pre-BCR is internalized and light-chain is recombined, allowing assembly of the mature BCR. Here, the BLNK/PLC γ 2 complex inhibits AKT activation and promotes differentiation. While loss of AKT activity allows cell differentiation to proceed, it also represents loss of an important pro-survival signal. Our model would suggest that transient expression of ROR1 at this stage of B-lineage differentiation offers an alternative mechanism for pro-survival signaling through activation of MEK/ERK (Figure 7B) (Taguchi et al., 2003). In the case of t(1;19) ALL, the t(1;19) lesion generates the E2A-PBX1 fusion product that contributes to the developmental arrest of B-cell progenitors at the pre-BII small stage of development. Expression and signaling of ROR1 and the pre-BCR complex are now retained in the malignant progenitor and provide onco-requisite signaling stimuli critical for the viability of these malignant cells. Abrogation of ROR1 signaling (with siRNA) results in inhibition of MEK/ERK activity leading to attenuation of AKT activity and impairment of cell viability (Figure 7C). Alternatively, inhibition of pre-BCR activity with dasatinib results in rapid inhibition of the PI3K/AKT pathway and results in loss of differentiation repression, abrogation of pro-proliferative signals, and subsequent impairment of viability. However, inhibition of the pre-BCR signaling complex also induces feedback activation of ROR1 expression and further activation of MEK/ERK signaling. In addition to partially supporting pro-survival signaling through MEK/ERK, ROR1 upregulation drives partial reactivation of AKT signaling resulting in rescue of cell viability (Figure 7D). As such, modulation of only ROR1 or only the pre-BCR is not as effective at killing t(1;19) cells as simultaneous antagonism of both pathways.

The optimal strategy for therapeutic targeting of ROR1 remains unclear. Immunological based therapies present a promising therapeutic strategy for specifically targeting ROR1-positive malignancies. Chimeric antigen receptor (CAR)-modified T-cells targeting B-cell lineage-specific surface markers, such as CD19 and CD20, are actively being investigated in clinical trials for B-cell malignancies (Porter et al., 2011; Till et al., 2008). Our data suggest that a similar strategy targeting ROR1 could prove valuable in treating most intermediate and mature B-cell malignancies. In fact, this strategy is already in development and showing

promising results against CLL and MCL samples (Hudecek et al., 2010). Further study addressing the potential toxicity of targeting ROR1 surface expression will be critical for advancing ROR1-targeting as a viable therapeutic option.

In conclusion, our work provides important evidence of ROR1 biological function in normal B-cell development and B-cell malignancy. It expands the pool of patients who could potentially benefit from ROR1 targeted therapy and has further suggested a high rate of overlap between the overexpression of ROR1 and sensitivity to the targeted kinase inhibitor dasatinib. Addition of t(1;19) and t(17;19) ALL as well as Burkitt's leukemia/lymphoma to the growing list of B-cell malignancies that exhibit ROR1 surface expression provides impetus for further study of ROR1 biology and ROR1-targeted therapies. Further, while dasatinib does not directly target ROR1, it does effectively reduce the viability of many ROR1-positive B-cell malignancies due to expression of the pre- or mature-BCR in these cells. Hence, our work would suggest further studies that may lead to implementation of dasatinib therapy for B-cell malignancies expressing the pre- or mature-BCR, which could also be supplemented with ROR1-directed therapies for enhanced efficacy.

EXPERIMENTAL PROCEDURES

Patient Samples

All clinical samples were obtained with informed consent with approval by the Institutional Review Board of Oregon Health & Science University and the Children's Oncology Group. Bone marrow mononuclear cells were separated on a Ficoll gradient. Cells were cultured in RPMI-1640 medium with 20% FBS (Atlanta Biologicals), L-glutamine, insulin/transferrin/sodium selenite, penicillin/streptomycin, fungizone (Invitrogen), and 10^{-4} M 2-mercaptoethanol (Sigma).

Primary leukemia cell xenograft

1×10^6 cells from a t(1;19) ALL patient bone marrow were inoculated via intra femoral injection into sublethally irradiated (250 cGy) NOD/SCID mice. When the mice became terminally ill due to overt leukemia, they were sacrificed and leukemia cells were harvested from bone marrow and spleen. Leukemic infiltration was confirmed by flow cytometry and cells were suspended in culture media (MEM-Alpha medium supplemented with 20% FBS, 1% penicillin/streptomycin, 1% Sodium-Pyruvate). For in vivo dasatinib treatment, 14 mice were injected with t(1;19)-positive ALL cells and left untreated for 8 days to allow cell engraftment. Mice were then divided into two groups and treated by oral gavage with dasatinib or vehicle control according to a dose escalating protocol, starting with 10 mg/kg daily for 6 days, 50 mg/kg once daily for 4 days, no treatment for 24 days, and 50 mg/kg twice daily thereafter. Mouse survival was monitored for 63 days. All mouse experiments were performed with approval by the Children's Hospital Los Angeles Institutional Animal Care and Use Committee.

Gene Expression Microarray

A meta-analysis was performed for gene expression microarray analyses of pediatric ALL patient samples and normal B-cell progenitor populations as previously described (Trageser et al., 2009). Datasets were processed and normalized using the RMA algorithm and normalization was validated based on even expression levels for a set of 7 reference genes (HPRT, COX6B, GUSB, GAPDH, PGK, ACTB and B2M) among all tissue samples studied. Gene expression values for the ROR1 probesets (211057_at and 205805_s_at) and the IGHM probeset (212827_at) were studied.

siRNA and Kinase Inhibitors

The RAPID assay and other siRNA experiments were performed as previously described (Tyner et al., 2009; Tyner et al., 2008). All siRNAs were from Thermo Fisher Scientific Dharmacon RNAi Technologies. Dasatinib and PD98059 were purchased from LC Labs, PCI-32765, BMS-599626, and ponatinib were purchased from Selleck, Doxorubicin was from Sigma, and the allosteric AKT inhibitor (published as drug #17 in Table 2 of (Bilodeau et al., 2008)) was provided by Merck Pharmaceuticals.

Immunoblotting

All immunoblotting was performed using standard protocols. For phospho-proteomic arrays, Proteome Profiler Human Phospho-Kinase Array assays (R&D Systems) were used and analyzed according to the manufacturer's protocol. Data was analyzed with ImageJ.

Statistical Analyses

For RAPID screens, the mean and standard deviation of all data points on the plate were computed and any data points exceeding two standard deviations of the mean plate value were considered significant. For cell viability, expression level, and phosphorylation state assays, a Student's t test was carried out for each drug dose or siRNA treatment compared with no drug control or non-specific siRNA, respectively. Xenograft mouse survival curves were analyzed using Log-rank (Mantel-Cox) test.

For further experimental details, see Supplemental Experimental Procedures.

Supplementary Material

Refer to Web version on PubMed Central for supplementary material.

Acknowledgments

We thank Cristina Tognon for helpful review of this manuscript. Patient samples from the Children's Oncology Group were obtained through a collaboration with the COG ALL Cell Bank (Proposal #2008-08). J.W.T. is supported by grants from the William Lawrence and Blanche Hughes Fund, the Leukemia & Lymphoma Society, the National Cancer Institute (5K99CA151457-02), and the Oregon Clinical and Translational Research Institute (OCTRI) grant number UL1 RR024140 from the National Center for Research Resources (NRCC), a component of the NIH, and NIH Roadmap for Medical Research. B.H.C. is supported by grants from the Oregon Child Health Research Center and by St. Baldricks Foundation. B.J.D. is an investigator of the Howard Hughes Medical Institute.

REFERENCES

- Baskar S, Kwong KY, Hofer T, Levy JM, Kennedy MG, Lee E, Staudt LM, Wilson WH, Wiestner A, Rader C. Unique cell surface expression of receptor tyrosine kinase ROR1 in human B-cell chronic lymphocytic leukemia. *Clin Cancer Res.* 2008; 14:396–404. [PubMed: 18223214]
- Bhuin T, Roy JK. Rab11 regulates JNK and Raf/MAPK-ERK signalling pathways during Drosophila wing development. *Cell Biol Int.* 2010; 34:1113–1118. [PubMed: 20642455]
- Bijl J, Sauvageau M, Thompson A, Sauvageau G. High incidence of proviral integrations in the Hoxa locus in a new model of E2a-PBX1-induced B-cell leukemia. *Genes Dev.* 2005; 19:224–233. [PubMed: 15655112]
- Bilodeau MT, Balitza AE, Hoffman JM, Manley PJ, Barnett SF, Defeo-Jones D, Haskell K, Jones RE, Leander K, Robinson RG, et al. Allosteric inhibitors of Akt1 and Akt2: a naphthyridinone with efficacy in an A2780 tumor xenograft model. *Bioorg Med Chem Lett.* 2008; 18:3178–3182. [PubMed: 18479914]
- Boulos N, Mulder HL, Calabrese CR, Morrison JB, Rehg JE, Relling MV, Sherr CJ, Williams RT. Chemotherapeutic agents circumvent emergence of dasatinib-resistant BCR-ABL kinase mutations

- in a precise mouse model of Philadelphia chromosome-positive acute lymphoblastic leukemia. *Blood*. 2011; 117:3585–3595. [PubMed: 21263154]
- Broome HE, Rassenti LZ, Wang HY, Meyer LM, Kipps TJ. ROR1 is expressed on hematogones (non-neoplastic human B-lymphocyte precursors) and a minority of precursor-B acute lymphoblastic leukemia. *Leuk Res*. 2011; 35:1390–1394. [PubMed: 21813176]
- Brunet A, Bonni A, Zigmond MJ, Lin MZ, Juo P, Ju LS, Anderson MJ, Arden KC, Blenis J, Greenberg ME. Akt promotes cell survival by phosphorylating and inhibiting a Forkhead transcription factor. *Cell*. 1999; 96:857–868. [PubMed: 10102273]
- Datta SR, Dudek H, Tao X, Masters S, Fu H, Gotoh Y, Greenberg ME. Akt Phosphorylation of BAD Couples Survival Signals to the Cell-Intrinsic Death Machinery. *Cell*. 1997; 91:231–241. [PubMed: 9346240]
- Dedera DA, Waller EK, LeBrun DP, Sen-Majumdar A, Stevens ME, Barsh GS, Cleary ML. Chimeric homeobox gene E2A-PBX1 induces proliferation, apoptosis, and malignant lymphomas in transgenic mice. *Cell*. 1993; 74:833–843. [PubMed: 8104101]
- Fukuda T, Chen L, Endo T, Tang L, Lu D, Castro JE, Widhopf GF 2nd, Rassenti LZ, Cantwell MJ, Prussak CE, et al. Antisera induced by infusions of autologous Ad-CD154-leukemia B cells identify ROR1 as an oncofetal antigen and receptor for Wnt5a. *Proc Natl Acad Sci U S A*. 2008; 105:3047–3052. [PubMed: 18287027]
- Gentile A, Lazzari L, Benvenuti S, Trusolino L, Comoglio PM. Ror1 is a pseudokinase that is crucial for met-driven tumorigenesis. *Cancer Res*. 2011; 71:3132–3141. [PubMed: 21487037]
- Hantschel O, Rix U, Schmidt U, Burckstummer T, Kneidinger M, Schutze G, Colinge J, Bennett KL, Ellmeier W, Valent P, Superti-Furga G. The Btk tyrosine kinase is a major target of the Bcr-Abl inhibitor dasatinib. *Proc Natl Acad Sci U S A*. 2007; 104:13283–13288. [PubMed: 17684099]
- Hashimoto S, Iwamatsu A, Ishiai M, Okawa K, Yamadori T, Matsushita M, Baba Y, Kishimoto T, Kurosaki T, Tsukada S. Identification of the SH2 domain binding protein of Bruton's tyrosine kinase as BLNK--functional significance of Btk-SH2 domain in B-cell antigen receptor-coupled calcium signaling. *Blood*. 1999; 94:2357–2364. [PubMed: 10498607]
- Herzog S, Reth M, Jumaa H. Regulation of B-cell proliferation and differentiation by pre-B-cell receptor signalling. *Nature Reviews Immunology*. 2009; 9:195–205.
- Hideshima T, Mitsiades C, Ikeda H, Chauhan D, Raje N, Gorgun G, Hideshima H, Munshi NC, Richardson PG, Carrasco DR, Anderson KC. A proto-oncogene BCL6 is up-regulated in the bone marrow microenvironment in multiple myeloma cells. *Blood*. 2010; 115:3772–3775. [PubMed: 20228272]
- Hsueh RC, Scheuermann RH. Tyrosine kinase activation in the decision between growth, differentiation, and death responses initiated from the B cell antigen receptor. *Adv Immunol*. 2000; 75:283–316. [PubMed: 10879287]
- Hudecek M, Schmitt TM, Baskar S, Lupo-Stanghellini MT, Nishida T, Yamamoto TN, Bleakley M, Turtle CJ, Chang WC, Greisman HA, et al. The B-cell tumor-associated antigen ROR1 can be targeted with T cells modified to express a ROR1-specific chimeric antigen receptor. *Blood*. 2010; 116:4532–4541. [PubMed: 20702778]
- Hunger SP. Chromosomal translocations involving the E2A gene in acute lymphoblastic leukemia: clinical features and molecular pathogenesis. *Blood*. 1996; 87:1211–1224. [PubMed: 8608207]
- Hunger SP, Galili N, Carroll AJ, Crist WM, Link MP, Cleary ML. The t(1;19)(q23;p13) results in consistent fusion of E2A and PBX1 coding sequences in acute lymphoblastic leukemias. *Blood*. 1991; 77:687–693. [PubMed: 1671560]
- Kamps MP, Baltimore D. E2A-Pbx1, the t(1;19) translocation protein of human pre-B-cell acute lymphocytic leukemia, causes acute myeloid leukemia in mice. *Mol Cell Biol*. 1993; 13:351–357. [PubMed: 8093327]
- Kamps MP, Look AT, Baltimore D. The human t(1;19) translocation in pre-B ALL produces multiple nuclear E2A-Pbx1 fusion proteins with differing transforming potentials. *Genes Dev*. 1991; 5:358–368. [PubMed: 1672117]
- Karaman MW, Herrgard S, Treiber DK, Gallant P, Atteridge CE, Campbell BT, Chan KW, Ciceri P, Davis MI, Edeen PT, et al. A quantitative analysis of kinase inhibitor selectivity. *Nat Biotechnol*. 2008; 26:127–132. [PubMed: 18183025]

- Krause DS, Van Etten RA. Tyrosine kinases as targets for cancer therapy. *N Engl J Med.* 2005; 353:172–187. [PubMed: 16014887]
- Li P, Harris D, Liu Z, Liu J, Keating M, Estrov Z. Stat3 activates the receptor tyrosine kinase like orphan receptor-1 gene in chronic lymphocytic leukemia cells. *PLoS One.* 2010; 5:e11859. [PubMed: 20686606]
- McCaig AM, Cosimo E, Leach MT, Michie AM. Dasatinib inhibits B cell receptor signalling in chronic lymphocytic leukaemia but novel combination approaches are required to overcome additional pro-survival microenvironmental signals. *Br J Haematol.* 2011; 153:199–211. [PubMed: 21352196]
- McWhirter JR, Neuteboom ST, Wancewicz EV, Monia BP, Downing JR, Murre C. Oncogenic homeodomain transcription factor E2A-Pbx1 activates a novel WNT gene in pre-B acute lymphoblastoid leukemia. *Proc Natl Acad Sci U S A.* 1999; 96:11464–11469. [PubMed: 10500199]
- Mendoza MC, Er EE, Blenis J. The Ras-ERK and PI3K-mTOR pathways: cross-talk and compensation. *Trends Biochem Sci.* 2011; 36:320–328. [PubMed: 21531565]
- Monroe JG. ITAM-mediated tonic signalling through pre-BCR and BCR complexes. *Nature Reviews Immunology.* 2006; 6
- Novak R, Jacob E, Haimovich J, Avni O, Melamed D. The MAPK/ERK and PI3K pathways additively coordinate the transcription of recombination-activating genes in B lineage cells. *J Immunol.* 2010; 185:3239–3247. [PubMed: 20709952]
- O'Hare T, Shakespeare WC, Zhu X, Eide CA, Rivera VM, Wang F, Adrian LT, Zhou T, Huang WS, Xu Q, et al. AP24534, a pan-BCR-ABL inhibitor for chronic myeloid leukemia, potently inhibits the T315I mutant and overcomes mutation-based resistance. *Cancer Cell.* 2009; 16:401–412. [PubMed: 19878872]
- Papavasiliou F, Jankovic M, Suh H, Nussenzweig MC. The cytoplasmic domains of immunoglobulin (Ig) alpha and Ig beta can independently induce the precursor B cell transition and allelic exclusion. *J Exp Med.* 1995; 182:1389–1394. [PubMed: 7595209]
- Park SY, Jin W, Woo JR, Shoelson SE. Crystal structures of human TBC1D1 and TBC1D4 (AS160) RabGTPase-activating protein (RabGAP) domains reveal critical elements for GLUT4 translocation. *J Biol Chem.* 2011; 286:18130–18138. [PubMed: 21454505]
- Sano H, Kane S, Sano E, Miinea CP, Asara JM, Lane WS, Garner CW, Lienhard GE. Insulin-stimulated phosphorylation of a Rab GTPase-activating protein regulates GLUT4 translocation. *J Biol Chem.* 2003; 278:14599–14602. [PubMed: 12637568]
- Taguchi T, Kiyokawa N, Mimori K, Suzuki T, Sekino T, Nakajima H, Saito M, Katagiri YU, Matsuo N, Matsuo Y, et al. Pre-B cell antigen receptor-mediated signal inhibits CD24-induced apoptosis in human pre-B cells. *J Immunol.* 2003; 170:252–260. [PubMed: 12496407]
- Teh YM, Neuberger MS. The immunoglobulin (Ig)alpha and Igbeta cytoplasmic domains are independently sufficient to signal B cell maturation and activation in transgenic mice. *J Exp Med.* 1997; 185:1753–1758. [PubMed: 9151700]
- Trageser D, Iacobucci I, Nahar R, Duy C, von Levetzow G, Klemm L, Park E, Schuh W, Gruber T, Herzog S, et al. Pre-B cell receptor-mediated cell cycle arrest in Philadelphia chromosome-positive acute lymphoblastic leukemia requires IKAROS function. *J Exp Med.* 2009; 206:1739–1753. [PubMed: 19620627]
- Tyner JW, Deininger MW, Loriaux MM, Chang BH, Gotlib JR, Willis SG, Erickson H, Kovacovics T, O'Hare T, Heinrich MC, Druker BJ. RNAi screen for rapid therapeutic target identification in leukemia patients. *Proc Natl Acad Sci U S A.* 2009; 106:8695–8700. [PubMed: 19433805]
- Tyner JW, Walters DK, Willis SG, Luttropp M, Oost J, Loriaux M, Erickson H, Corbin AS, O'Hare T, Heinrich MC, et al. RNAi screening of the tyrosine kinome identifies therapeutic targets in acute myeloid leukemia. *Blood.* 2008; 111:2238–2245. [PubMed: 18025156]
- Wang Z, Pedersen E, Basse A, Lefever T, Peyrollier K, Kapoor S, Mei Q, Karlsson R, Chrostek-Grashoff A, Brakebusch C. Rac1 is crucial for Ras-dependent skin tumor formation by controlling Pak1-Mek-Erk hyperactivation and hyperproliferation in vivo. *Oncogene.* 2010; 29:3362–3373. [PubMed: 20383193]

Williams DL, Look AT, Melvin SL, Roberson PK, Dahl G, Flake T, Stass S. New chromosomal translocations correlate with specific immunophenotypes of childhood acute lymphoblastic leukemia. *Cell*. 1984; 36:101–109. [PubMed: 6607116]

\$watermark-text

\$watermark-text

\$watermark-text

HIGHLIGHTS

- ROR1 and the pre-BCR are therapeutic targets for t(1;19)-ALL cells
- t(1;19)-ALL cells are universally sensitive to dasatinib due to pre-BCR inhibition
- ROR1 and the pre-BCR drive cooperative signaling cascades
- Silencing of ROR1 accentuates dasatinib killing of t(1;19)-ALL cells

\$watermark-text

\$watermark-text

\$watermark-text

SIGNIFICANCE

The 1;19-translocation is one of the most common recurring chromosomal abnormalities in acute lymphoblastic leukemia (ALL). We have identified a therapeutic gene target, ROR1, for t(1;19)-ALL. We have also identified a kinase inhibitor, dasatinib, with universal efficacy against t(1;19)-ALL cells due to inhibition of the pre-B-cell receptor (pre-BCR) – another oncorequisite pathway for t(1;19)-ALL. These phenotypes are recapitulated in other ALL cells of intermediate developmental stage such as t(17;19)-ALL as well as mature B-cell malignancies such as t(8;14)-Burkitt's. Finally, we have identified signaling pathways downstream of ROR1, which cooperate with pre-BCR signaling. Our findings highlight a functional link between the pre-BCR and ROR1 and the importance of inhibiting both pathways to augment tumor cell killing.

\$watermark-text

\$watermark-text

\$watermark-text

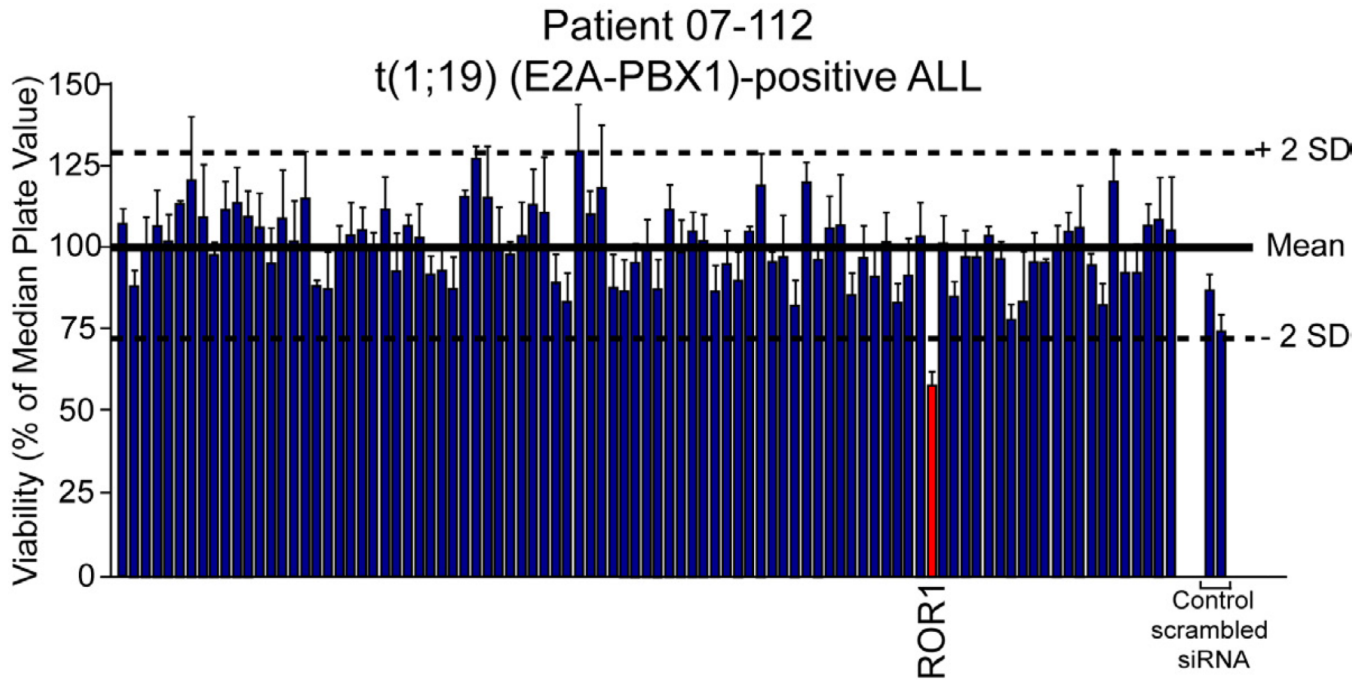


Figure 1. ROR1 is a functional target in t(1;19) ALL

White Blood cells (2.25×10^7) from a t(1;19)-positive ALL patient (07-112) were suspended in siPORT buffer and incubated with 1 μ M siRNA from an siRNA library individually targeting each member of the tyrosine kinase family as well as N-RAS, K-RAS, and single and pooled non-specific siRNA controls. Cells were electroporated on a 96-well electroporation plate at 1110 V (equivalent of 150 V), 200 μ sec, 2 pulses. Cells were replated into culture media and cell viability was determined by addition of a tetrazolium salt (MTS assay) at day 4 post-electroporation. Values represent percent mean (normalized to the median value on the plate) \pm s.e.m (n = 3). See also Figure S1.

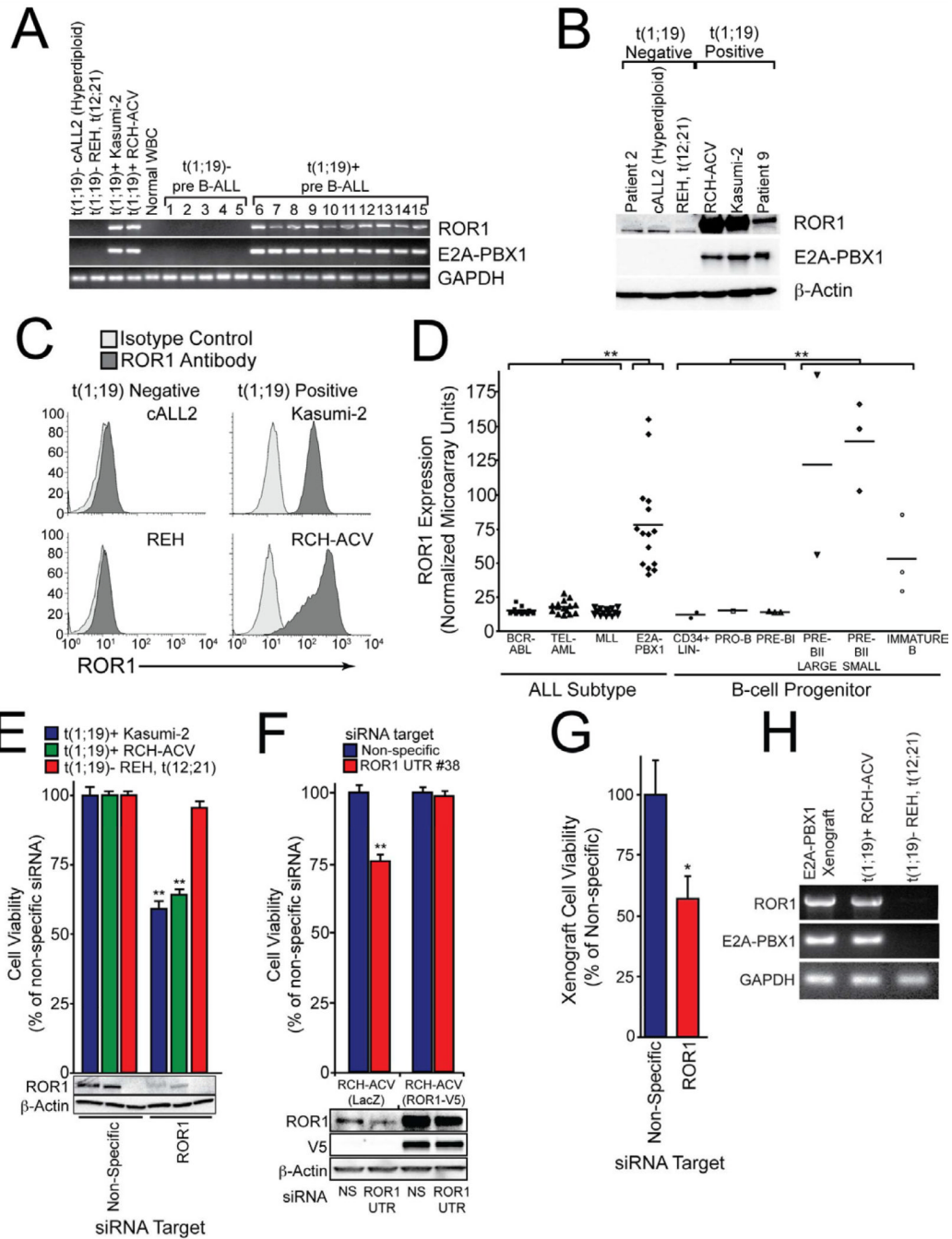


Figure 2. ROR1 is universally expressed and a therapeutic target in t(1;19) ALL
(A) cDNA derived from t(1;19)-positive and negative cell lines and primary patient samples was amplified using primers specific for ROR1, E2A-PBX1, or GAPDH and PCR products were analyzed by gel electrophoresis.
(B) Whole cell extracts derived from t(1;19)-positive and negative cell lines and primary patient samples were subjected to immunoblot analysis using antibodies specific for ROR1, E2A-PBX1, or β-Actin.

(C) Flow cytometric analysis of t(1;19)-positive and negative cell lines was performed using specific polyclonal anti-human ROR1 antibodies (dark grey histogram) versus isotype control (light grey histogram).

(D) Gene expression microarray data for pediatric ALL patients and normal B-cell progenitor populations were compiled into a meta-analysis. Patients with MLL gene rearrangements, t(9;22) (BCR-ABL), t(12;21) (TEL-AML), or t(1;19) (E2A-PBX1) (n=15 for each subset) and non-malignant B-cell progenitor populations (CD34+ Lin-, pro-B, pre-B, pre-BII large, pre-BII small, and immature B) (n=15 total) were examined and Affymetrix intensity values for ROR1 are plotted for each individual patient sample. (**p < 0.01)

(E) RCH-ACV or Kasumi-2 cells (both t(1;19)-positive) as well as REH cells (t(12;21)-positive) were electroporated in the presence of non-specific or ROR1-targeting siRNA and plated into culture media. After 3 days, a sample of cells was harvested for immunoblot analysis using antibodies specific for ROR1 or β -Actin. After 4 days, cells were subjected to an MTS assay to measure cell viability. Values represent percent mean (normalized to non-specific control wells) \pm s.e.m. (n = 10). (**p < 0.01)

(F) RCH-ACV cells stably expressing ROR1-V5 or LacZ control were electroporated in the presence of non-specific or ROR1 UTR-targeting siRNA and plated into culture media. After 3 days, a sample of cells was harvested for immunoblot analysis using antibodies specific for ROR1, V5, or β -Actin. After 4 days, cells were subjected to an MTS assay to measure cell viability. Values represent percent mean (normalized to non-specific control wells) \pm s.e.m. (n = 6). (**p < 0.01)

(G) Primary cells from a t(1;19) ALL patient were propagated in NOD-SCID mice lacking the IL-2 receptor γ chain. Xenograft cells were harvested from bone marrow and spleen of overtly leukemic mice and electroporated with non-specific or ROR1-targeting siRNA. After 4 days, cells were subjected to an MTS assay to measure cell viability. Values represent percent mean (normalized to non-specific control wells) \pm s.e.m. (n = 4). (*p < 0.05)

(H) Primary cells from a t(1;19) ALL patient were propagated in a xenograft mouse model as above and RNA was harvested from cell extracts. PCR was performed on cDNA with primers specific for ROR1, E2A-PBX1, or GAPDH. The t(1;19) positive (RCH-ACV) and negative (REH) cell lines were included for comparison. See also Figure S2.

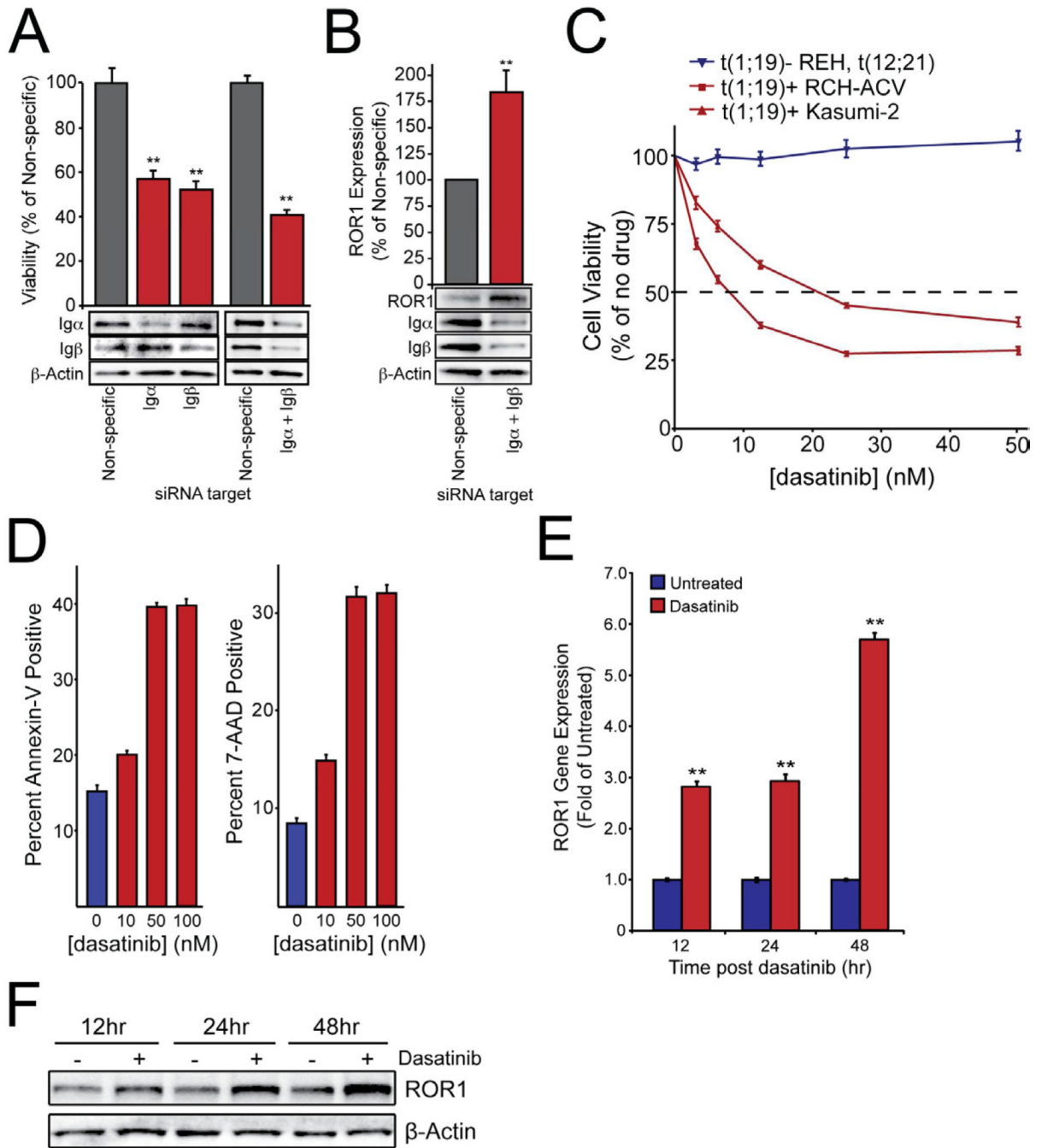


Figure 3. Pre-BCR signaling inhibition impairs t(1;19) cell viability and activates ROR1 expression

(A) RCH-ACV cells were electroporated in the presence of non-specific siRNA or siRNA targeting Ig α , Ig β , or both and then plated in culture media. After 3 days, a sample of cells was harvested for immunoblot analysis using antibodies specific for Ig α , Ig β , or β -Actin. After 4 days, cells were subjected to an MTS assay to measure cell viability. Values represent percent mean (normalized to non-specific control wells) \pm s.e.m. (n = 6). (**p < 0.01)

(B) RCH-ACV cells were electroporated in the presence of non-specific or Ig α and Ig β -targeting siRNA and then plated in culture media. After 3 days, cells were harvested for

immunoblot analysis using antibodies specific for ROR1, Ig α , Ig β , or β -Actin. One representative blot is included. Densitometry was performed to quantitate ROR1 expression. Values represent percent mean (normalized to non-specific control) \pm s.e.m. (n = 3). (**p<.01)

(C) RCH-ACV, Kasumi-2, and REH cells were cultured in graded concentrations of the kinase inhibitor dasatinib for 3 days at which time cells were subjected to an MTS assay for measurement of cell viability. Values represent percent mean (normalized to no-drug control wells) \pm s.e.m. (n = 6).

(D) RCH-ACV cells were cultured in graded concentrations of dasatinib for 96 hours before being stained with Annexin-V PE and 7-AAD and analyzed by flow cytometry to determine induction of apoptosis. Values represent the percentage of total positive cells \pm s.e.m. (n = 3). (*p<.05, **p<.01).

(E and F) RCH-ACV cells were cultured in the presence of 100nM dasatinib for 12, 24, and 48 hours. Cells were collected for RNA harvest and quantitative PCR analysis **(E)** or lysed for immunoblot analysis **(F)**. PCR was performed on cDNA with primers specific for ROR1 and GAPDH to determine relative ROR1 mRNA expression levels. Values represent the fold change (normalized to untreated control cells) \pm s.e.m. (n = 6). (**p<.01).

Immunoblotting was performed with antibodies specific for ROR1 or β -Actin to determine relative ROR1 protein expression. See also Figure S3.

\$watermark-text

\$watermark-text

\$watermark-text

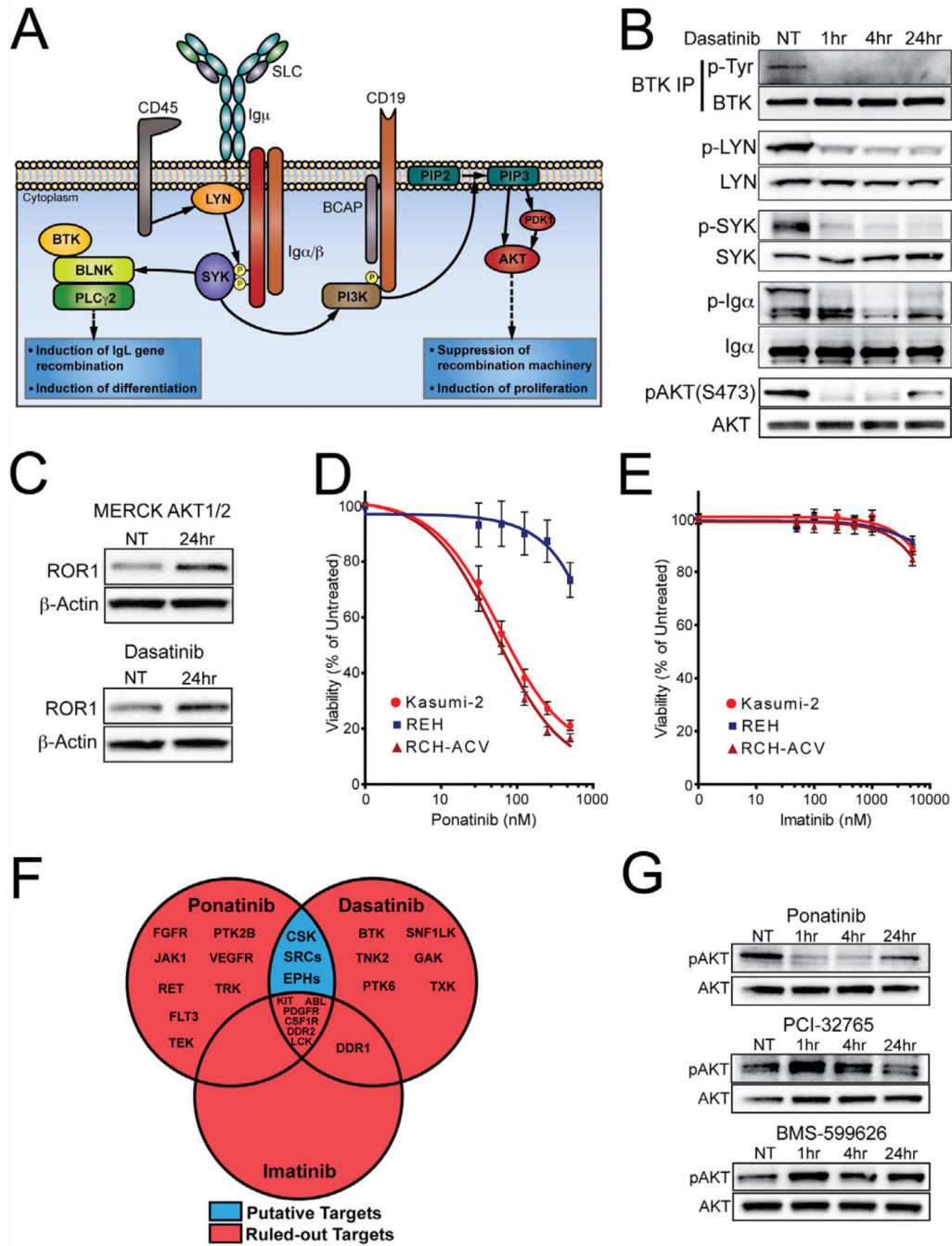


Figure 4. Dasatinib inhibits pre-BCR/SRC/AKT signaling and upregulates ROR1 in t(1;19) ALL
(A) Schematic of pre-BCR signaling and function during pre-B development. Adapted from (Herzog et al., 2009; Monroe, 2006)
(B) RCH-ACV cells were treated with dasatinib (50 nM) over a time course and whole cell extracts were subjected to immunoblot analysis for total or phospho-LYN, SYK, Ig α , and AKT. In addition, BTK was immunoprecipitated from the same cellular lysates and immunoprecipitates were immunoblotted for total or phospho-BTK.

(C) RCH-ACV cells were treated with an allosteric inhibitor of AKT (1 μ M) or dasatinib (100nM) for 24 hours and whole cell extracts were subjected to immunoblot analysis for ROR1 and β -Actin.

(D and E) RCH-ACV, Kasumi-2, and REH cells were cultured in graded concentrations of the kinase inhibitors ponatinib (D) or imatinib (E) for 3 days at which time cells were subjected to an MTS assay for measurement of cell viability. Values represent percent mean (normalized to no-drug control wells) \pm s.e.m. (n = 6).

(F) Venn-diagram identifies potential phenotype-mediated targets of dasatinib (CSK, SRC-family kinases, EPH receptors). Binding constants: dasatinib (<10nM), ponatinib (<25nM), imatinib (<500nM) (O'Hare et al, 2009; Karaman et al, 2008).

(G) RCH-ACV cells were treated with ponatinib (50nM), PCI-32765 (50nM), or BMS-599626 (500nM) over a time course and whole cell extracts were subjected to immunoblot analysis for total or phospho-AKT. See also Figure S4.

\$watermark-text

\$watermark-text

\$watermark-text

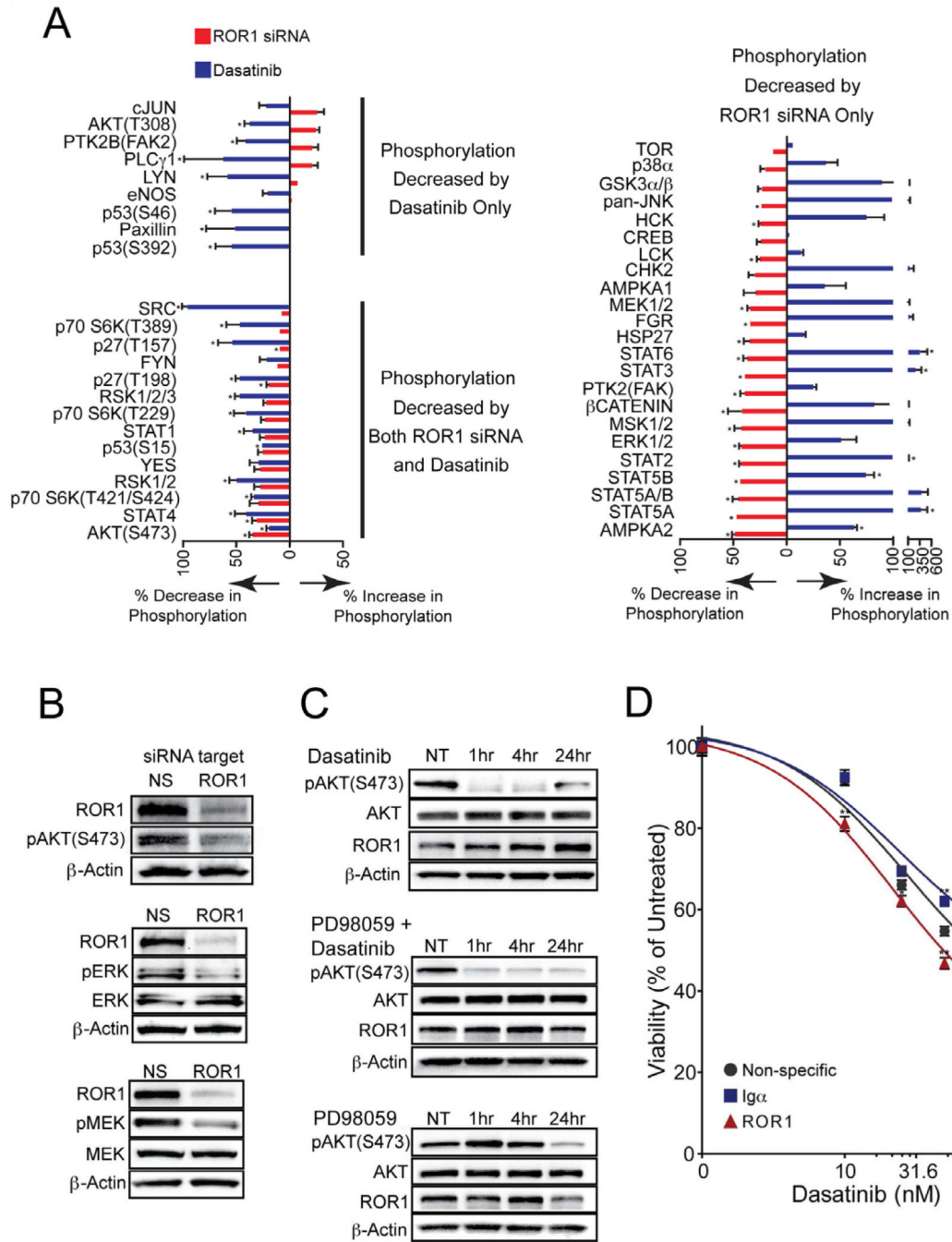


Figure 5. Inhibition of pre-BCR or ROR1 result in counter-balancing effects on signaling
(A) RCH-ACV cells were treated with dasatinib for 24 hours or ROR1 siRNA for 72 hours and whole cell extracts were analyzed by phospho-proteomic array. Values on the graph represent percent phosphorylation change \pm s.e.m. ($n = 3$) ($*p < .05$) of a total of 46 phosphoproteins for dasatinib relative to cells in the absence of any drug and for ROR1 siRNA relative to cells transfected with non-specific siRNA.
(B) RCH-ACV cells were transfected with ROR1 or non-specific siRNA for 72 hours and whole cell extracts were subjected to immunoblot analysis for ROR1, phospho-AKT at residue Serine 473 and β -Actin; ROR1, total and phospho-ERK, and β -Actin; ROR1, total

and phospho-MEK, and β -Actin for validation of ROR1 modulation observed by the phospho-proteomics screen in (A).

(C) RCH-ACV cells were treated with dasatinib (50nM), PD98059 (50 μ M), or both over a time course and whole cell extracts were subjected to immunoblot analysis for total or phospho-AKT at residue Serine 473, ROR1, and β -Actin.

(D) RCH-ACV cells were electroporated in the presence of non-specific, ROR1-targeting, or I γ α -targeting siRNA and then plated in culture media. After 2 days, graded concentrations of dasatinib were added. Cells were allowed to culture an additional 2 days before they were subjected to an MTS assay for measurement of cell viability. Values represent percent mean (normalized to no-drug control wells) \pm s.e.m. (n = 5). (*p<.05, **p<.01). See also Figure S6.

\$watermark-text

\$watermark-text

\$watermark-text

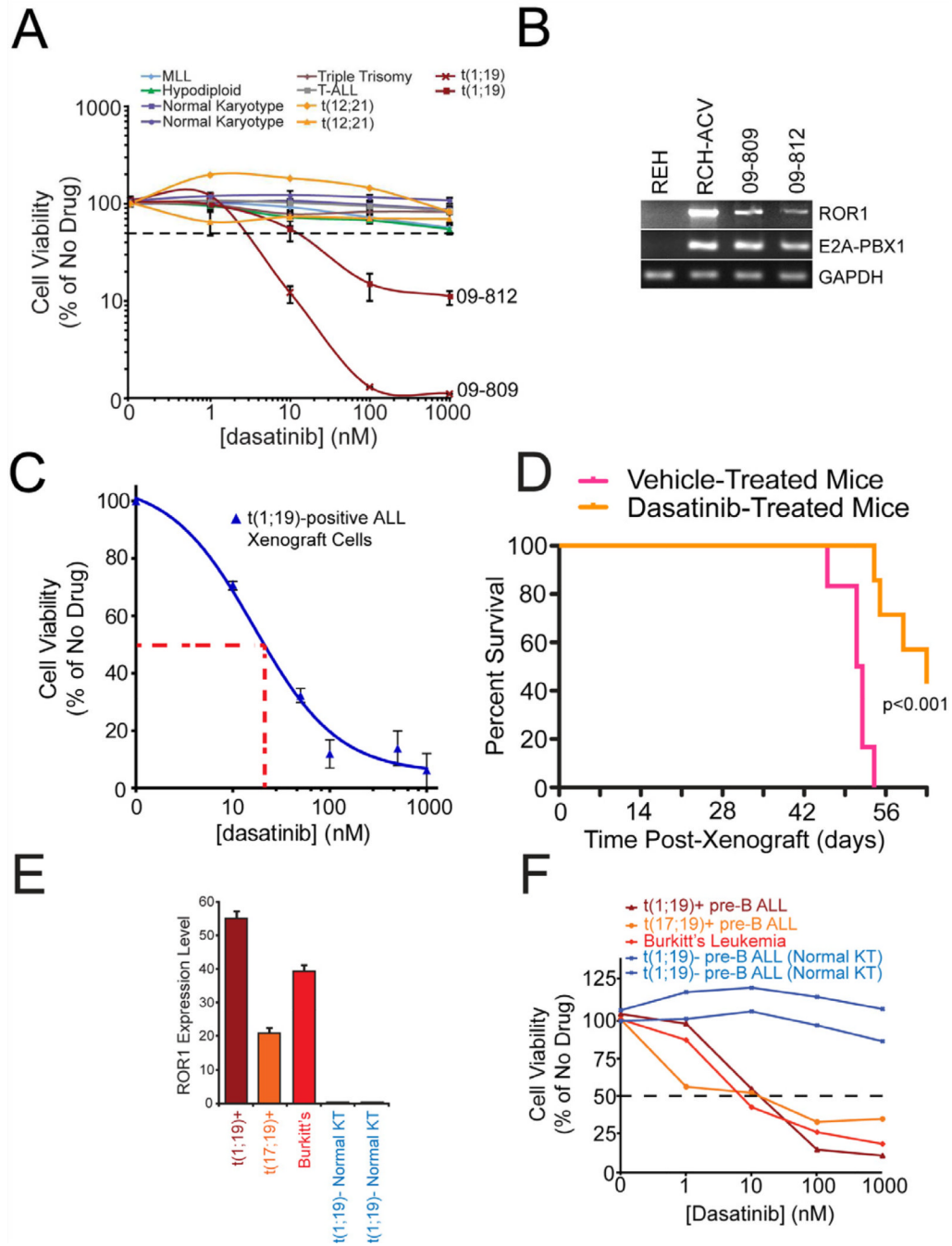


Figure 6. Clinical significance of dasatinib sensitivity in pre-BCR/BCR-positive malignancies
(A) Malignant cells from 10 pediatric ALL patients exhibiting a variety of chromosomal translocations (2 positive for t(1;19)) were cultured in graded concentrations of the kinase inhibitor, dasatinib, for 3 days at which time cells were subjected to an MTS assay for measurement of cell viability. Values represent percent mean (normalized to no-drug control wells) \pm s.e.m. (n = 3).
(B) cDNA derived from primary samples of t(1;19) ALL patients 09-809 and 09-812 was amplified using primers specific for ROR1, E2A-PBX1, or GAPDH. The t(1;19) positive (RCH-ACV) and negative (REH) cell lines were included for comparison.

(C) Early passage t(1;19) ALL xenograft cells (ICN12) were cultured in graded concentrations of the kinase inhibitor dasatinib for 3 days at which time cells were subjected to an MTS assay for measurement of cell viability. Values represent percent mean (normalized to no-drug control wells) \pm s.e.m. (n = 4).

(D) Early passage t(1;19) ALL xenograft cells (ICN12) were injected intravenously into NOD/SCID mice. Mice were left untreated for 8 days to allow engraftment of cells and subdivided into two groups, one treated with dasatinib and the other with vehicle control. An initial dose-escalating round of treatment commenced with 10 mg/kg dasatinib for 6 days, followed by 50 mg/kg dasatinib for 4 days. Mice were untreated for the following 24 days, and this was followed by 12 additional days of dasatinib or vehicle treatment. Mouse survival was monitored over the course of the treatment.

(E) cDNA derived from t(1;19) ALL, t(17;19) ALL, Burkitt's lymphoma, and normal karyotype ALL primary samples was analyzed for relative ROR1 mRNA expression using quantitative PCR. cDNA was amplified using primers specific for ROR1 and GAPDH, and ROR1 levels were normalized to GAPDH. Values represent mean arbitrary quantitative PCR units \pm s.e.m. (n = 3).

(F) t(1;19) ALL, t(17;19) ALL, Burkitt's lymphoma, and normal karyotype primary samples were cultured in the presence of graded concentrations of dasatinib. After 3 days, cells were subjected to an MTS assay for measurement of cell viability. Values represent percent mean, normalized to no-drug control wells. See also Figure S7.

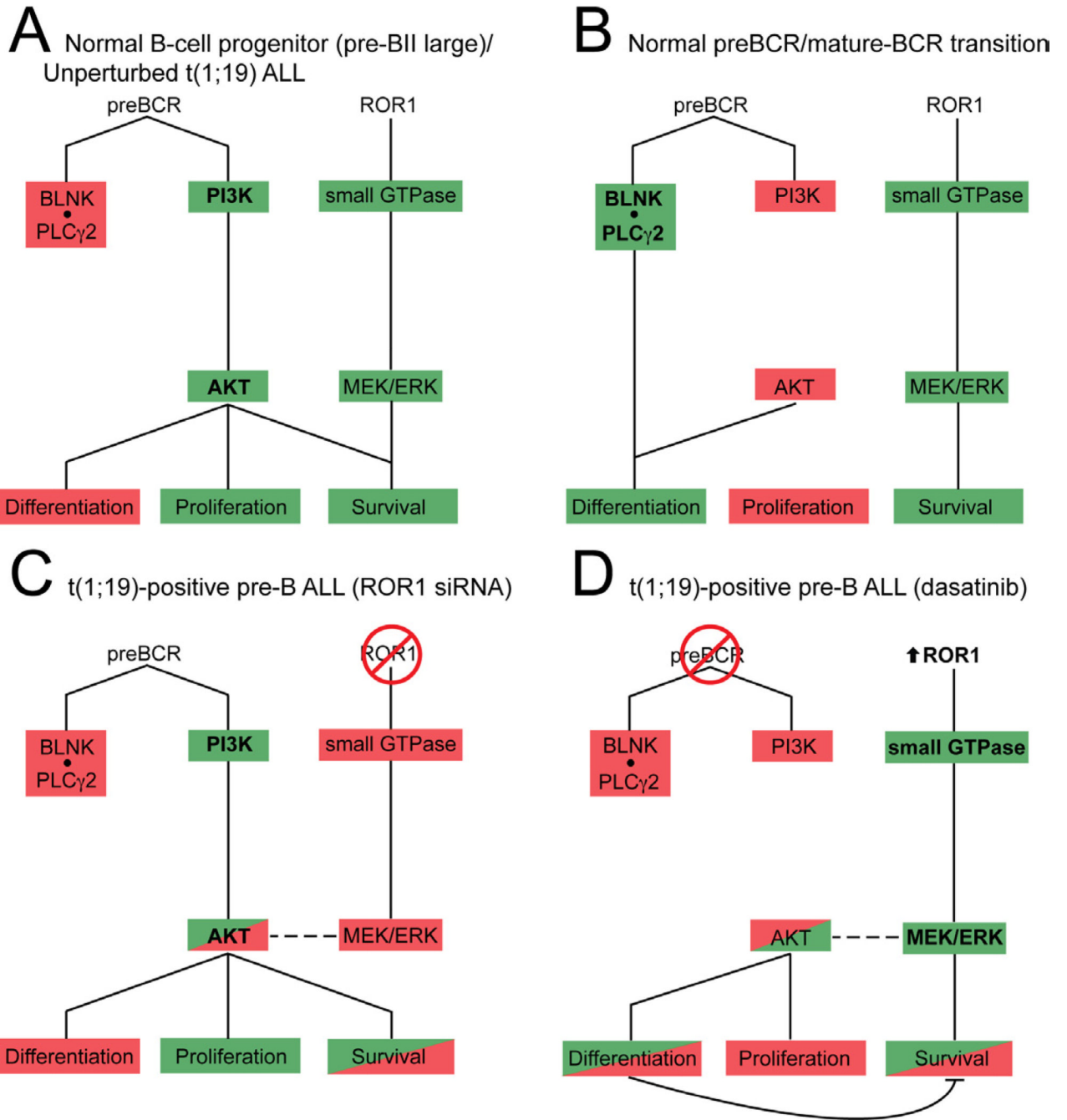


Figure 7. Model for ROR1 supported B-cell development and crosstalk between ROR1 and the pre-BCR during therapeutic modulation of t(1;19) ALL
 Schematic of ROR1 and pre-BCR signaling network and function during normal B-cell development and t(1;19)-positive pre-B ALL. Green indicates active signaling; red indicates inhibited signaling.

\$watermark-text

\$watermark-text

\$watermark-text

Table 1

ROR1 Associated Proteins in t(1;19) ALL

Lysates from the t(1;19)-positive ALL cell lines (Kasumi-2, 697, and RCH-ACV) were subjected to immunoprecipitation with ROR1-specific antibody or an isotype matched control. Immunoprecipitates were then analyzed by mass spectrometry (MS). All proteins that were identified at a similar frequency in isotype controls as ROR1-specific antibody samples were considered to be non-specific interactions and eliminated. Only proteins that were identified with ROR1 antibody and not with isotype control were considered as candidate ROR1-interacting proteins. Genes name, UniProt Accession number, and corrected MS/MS spectral counts are shown for each identified protein as well as β -Actin control. See also Figure S5.

Gene	Accession #	Isotype Control			ROR1 Antibody		
		Kasumi-2	697	RCH-ACV	Kasumi-2	697	RCH-ACV
ROR1	Q01973	0	0	0	30	28	19
TRIM21	P19474	0	0	0	12	0	12
MORC3	Q14149	0	0	0	7	17	18
TBC1D1	Q86TI0	0	0	0	9	1	3
TBC1D4	O60343	0	0	0	9	0	2
ACTB	P60709	15	23	26	8	47	26